Water and Soil Management and Modeling

Online ISSN: 2783 - 2546

University of Mohaghegh Ardabili

Optimal Channel Geometry for Balancing Discharge and Tidal Resistance: Insights from the Shatt al-Arab River

R. Jawad Karrar. [1], **Hirad Abghari** [2*]

[1] PhD student of Watershed Management Sciences and Engineering, Department of Range and Watershed Management, Faculty of Natural Resources, Urmia University, Iran
[2] Associate Professor, Department of Range and Watershed Management, Faculty of Natural Resources, Urmia University, Iran

Abstract

Cross-sectional geometry has a fundamental impact on the hydraulic behavior of the Shatt al-Arab River, an important waterway providing the water life supply to almost 4.5 million people in Basra City, southern Iraq. Using 200 cross sections at 1-km spacing through a 200-km hydrodynamic modeling framework that is employed in HEC-RAS, the analysis combines Sentinel-2 and Landsat-9 satellite imagery, 30-m DEM datasets, and in situ discharge measurements to quantify the impact of channel width on flow velocity, tidal intrusion, and sediment dynamics. Here, we find an inverse relationship between channel width and flow velocity ($R^2 = 0.92$). In this way, expansion of 150 to 350 m of channel increases discharge capacity by 125% but at the same time, flow velocity decreases by 57%, increasing tidal penetration by half while increasing the sediment deposition by 50%. In contrast, channel narrowing results in high water levels with a rise in flood risk of up to 1.8 m. An optimal width range of 280–300 m is determined which provides a balanced hydraulic performance in terms of discharge capacity, approximately 5,900 m^3/s capacity, seawater intrusion by ~25 km, and sediment build-up by nearly 35% as opposed to the wide channel segments. The results suggest that this width of channel should be considered an optimal width range for river rehabilitation and management, with dredging of high-sedimentation reaches (100–150 km; >12 cm/year) be in the priority mode. The continued and real-time hydrological monitoring application is further recommended in order to assure sustainable water security, with long-term river operation.

Keywords: Estuarine hydraulics, River geometry optimization, Salinity intrusion, HEC-RAS modeling, Sediment transport, Shatt al-Arab River

Article Type: Research Article
Academic Editor: Raoof Mostafazadeh

[*]Corresponding Author, E-mail: h.abghari@urmia.ac.ir
Citation: Karrar, R. J., Abghari, H. (2026). Optimal Channel Geometry for Balancing Discharge and Tidal Resistance: Insights from the Shatt al-Arab River. Water and Soil Management and Modelling, 6(2) (Special Issue: New Approaches to Water and Soil Management and Modeling), 267-286.
doi: 10.22098/mmws.2026.19094.1754
Received: 20 December 2025, Received in revised form: 09 January 2026, Accepted: 23 January 2026, Published online: 03 June 2026
Water and Soil Management and Modeling, Year 2026, Vol. 6, No.2 (Special Issue), pp. 267-286
Publisher: University of Mohaghegh Ardabili

1. Introduction.

The Shatt al-Arab River (30.4°N, 48.2°E), created from the confluence of the Tigris and Euphrates Rivers in Al-Qurna, supplies the local freshwater to 4.5 million inhabitants in Basra, southern Iraq (Al-Saadi, 1989). The Shatt al-Arab River, longer than 200 km long, with channel widths between 200 and 1,500 m, is a highly dynamic tidal estuary with the interaction of fluvial and marine processes accounting for significant hydrodynamics and geomorphology variation (Khalifa, 2012). Significant changes have taken place in the river, the worst being declining upstream flows (850 → 300 m^3/s; Hadi et al., 2021), Salinity intrusion exceeding freshwater thresholds under reduced discharge has been widely documented in tide-dominated rivers (Savenije, 2012; Buschman et al., 2010) and rising sedimentation of 18 cm/year in the river's lower reaches. These pressures and climate change stem from anthropogenic imperatives -- primarily extensive upstream damming, insufficient wastewater treatment, and climate change-- and they collectively affect agriculture, public health, and navigation (Passeri et al., 2015; Al-Taie and Saleh, 2020). One important, yet largely unexplored aspect of this deterioration is cross sectional geometry variation. Channel width and depth gradients induced by factors such as erosion, sedimentation and engineering affect the river's hydraulic response to tidal forcing – well recorded in other global estuaries (Julien, 2002; Mahdi et al., 2021 The Shatt al-Arab estuary is in the midst of multi-stage hydrological failure for two reasons: dramatic decreases in freshwater volume and increased tidal contribution from the Persian Gulf. Tigris–Euphrates discharge was down considerably—from nearly 850 to about 300 m^3/s after the construction of the Ilisu Dam (Hadi et al., 2021)—this has caused the river to have a much-diminished natural ability to become increasingly dilute and absorb more marine forces. Accordingly, currents that produce tidal water in the basin have become the principal transportation agent of salinity to the landward land column, which is often regarded as a secondary hydraulic contribution to flooding (Ralston & Geyer, 2019; Al-Abbadi, 2023). The Shatt al-Arab is facing an 'estuarine squeeze', a phenomenon where the reduction in freshwater discharge from upstream (Tigris and Euphrates) and the increasing tidal influence from the Persian Gulf compress the freshwater-seawater mixing zone. This process accelerates salinity intrusion into critical agricultural areas and municipal water intakes in Basra. Which is associated with decreased river discharge and increased marine forcing, driving salinity levels above 5,000 ppm in critical water supplies and agricultural regions. Consequently, approximately 74% of land cultivated in Al-Faw has been converted into saline sabkhas (Khodair, 2024). Adding to the environmental stresses are longstanding governance and transboundary management issues in the basin (El-Fadel et al., 2002; UNESCWA, 2023). The estuary hydraulic response is influenced, in a three-factor way by cross-sectional geometry for flow resistance, tidal penetration and depositional processes. Firstly, large channel widening (>500 m) corresponds to lower flow velocities (≤0.5 m/s), leading to longer periods of saline water retention and deeper inland intrusion (Van Rijn, 1984). Second, low-speed areas - particularly the ones within the region from the 100 km to 150 km scale - favor sediment uptake at a rate between 12 to 18 cm/year (Al-Mudhafar & Al-Aboodi, 2022), thus diminishing hydraulic conveyance. Third, narrower channel widths (<250 m) tend to heighten flood peaks by 1.8 m, hence heightening flood risks (Jassim & Saleh, 2019). Such patterns are in keeping with the theory on alluvial hydraulic geometries (Julien, 2002): channel width shows a predictable relationship with discharge as shown in the plot ($W \propto Q^{0.5}$), and is responsible for approximately 92% of variance in velocity ($p < 0.01$). Other systems using international estuaries have shown similar results such as the Mekong Delta, where changes to width resulted in a 40% increased tidal energy (Mahdi et al., 2021). Although earlier works have yielded valuable information on tidal intrusion—such as mapping inland penetration up to 100 km

using HEC-RAS (Al-Taie & Saleh, 2020) and identifying sediment hotspots over 3 m near Abu Al-Khasib (Al-Mudhafar & Al-Aboodi, 2022)—there are still several important research gaps. Significantly, no published study has quantitatively analyzed channel width, discharge efficiency, salinity reduction, and sediment balance as tradeoffs. Furthermore, local hydrodynamic models are rarely able to account for basin-scale effects of upstream Turkish and Iranian dams, and most analyses use bathymetric datasets that are post-2015 with uncertainties above ±15%. Those constraints limit the construction of a comprehensive, evidence-based framework for the rehabilitation of one of Iraq's essential waterways. The Shatt al-Arab River primary water resource for 4.5 million residents in Basra, is undergoing a critical destabilization of its hydraulic equilibrium due to the persistent decline in freshwater inflows from upstream Tigris–Euphrates sources. This hydrological stress has led to impaired discharge efficiency, accelerated sedimentation, and intensified tidal intrusion. Despite existing research, significant knowledge gaps persist regarding the process-based evaluation of tidal propagation regulated by cross-sectional variability, the efficiency of sediment transport under diverse geometric conditions, and the complex hydraulic trade-offs between flow velocity, flood risk, and discharge capacity. These gaps currently impede the development of geometry-informed management strategies. To address this, the present study employs HEC-RAS hydrodynamic modeling to determine the geometric controls governing discharge capacity, tidal reach, and sediment flux. By interrogating how shifting cross-sectional geometry alters the river's hydraulic characteristics, this research seeks to identify the optimal configuration for enhanced hydraulic stability and water security under contemporary stresses. These findings establish a critical empirical framework for rehabilitation, dredging operations, and the design of hydraulic structures, providing essential support for sustainable, climate-resilient water resource management in the region

2. Materials and Methods

2.1. Study Area:

The study region is the Shatt al-Arab River (called Arvand Rud in Persian), located in southern Iraq in Basra (Figure 1).

Figure 1. Geographic location of the Shatt Al-Arab River, Basra, Southern Iraq (2025). The inset map (a) shows the regional context within Iraq, while (b) provides the detailed study area geometry. Source: Multi-sensor satellite data (Sentinel-2/Landsat-9) validated via DEM datasets.

Study Objectives to incorporate the HEC-RAS into the study to investigate influence of variation in the Shatt al-Arab river's cross-sectional distance on water discharge and tidal propagation.

1. Use accurate topographic measurements to identify longitudinal shifts in river width.
2. Evaluate the quantitative effects of these changes on flow speed, discharge capacity, and tidal waves. Establish an engineering standard for a proposed cross-section design that should capture an ideal cross-section for a gradual reduction in the discharge. The hydraulic response of Shatt al-Arab River to a 200 km stretch was analyzed with multi-source, integrated multiscale approaches using a multi-source, integrated methodology approach. The workflow employed satellite geomorphological extraction, geospatial verification, hydrodynamic modeling and spatial analytics as well as hydrodynamic modeling in a multistage analysis to estimate the impact of cross-sectional variation on water flow and tidal response.

2.2. Data Sources and Preprocessing Satellite and Elevation Data. High-resolution multispectral images were collected from Sentinel-2 (10 m) and Landsat-9 (15–30 m) to ascertain active channel margins, water surface extents and platform adjustments. To set vertical reference and detect bank elevations and cross-sectional geometry, the Digital Elevation Model (DEM)—30 m—was employed. Horizontal positional accuracy (<10 m) was maintained through the orthorectification of Sentinel-2 imagery. Vertical accuracy (<0.5 m) was ensured by calibrating the 30-m DEM with 15 physical benchmark surveys and in-situ cross-sectional depth measurements provided by the Ministry of Water Resources to ensure a precise representation of the riverbed topography.

Hydrological and Tidal information was collected for the years 2010–2020 for the Al-Faw hydrological station from Ministry of Water Resources in Iraq, the most continuously available dataset of downstream boundary forcing. Discharge data for the Tigris and Euphrates rivers were extracted from official hydrological monitoring station records, incorporating the downstream impacts of upstream dam construction, specifically the 'Ilisu Dam.' The hydrological inputs were further calibrated and cross-referenced with the UNESCWA (2023) report on transboundary water resources to ensure data reliability. Geospatial Verification and Cross-Sectional Extraction: A total of 200 cross-sections were digitized from orthorectified aerial imagery at 1-km intervals. These data were subsequently refined and integrated using ArcGIS to ensure high spatial accuracy and morphological consistency Validation:

1. Flow-axis correction to reduce the geometric distortion, caused by channel curvature.

2. Development of active bankfull boundaries using Normalized Difference Water Index (NDWI) and supervised classification to avoid artificial widening or narrowing by restricting to the actual bank full using NDWI and supervised classification to reduce the artificial widening and/or narrowing effects.

3. Vertical reconciliation between the profile and DEM elevations that were derived from the images to ensure consistency across different spatial datasets.

4. Error minimization, i.e. minimization of positional uncertainties of <10 m horizontal, <0.5 m vertical.

The geometrical input of HEC-RAS reflected that the river was in proper morphologic condition at that time. Hydrodynamic Model Setup: HEC-RAS 6.3.1. A one-dimensional unsteady-flow model was developed using HEC-RAS 6.3.1. The model domain encompasses a 200-km reach, discretized into 200 cross-sections with a uniform spacing of 1 km to ensure high spatial resolution. To simulate sediment dynamics, the HEC-RAS Sediment Module was activated using the Ackers-White transport function, selected for its reliability in estuarine environments with fine-grained bed material ($d_{50} \approx 0.04$ mm). Boundary conditions included a flow hydrograph at the upstream end and a tidal stage hydrograph at the downstream Al-Faw station. Roughness Parameterization of Manning's. Manning's n

has a detailed classification was assigned based on: • Bank vegetation density. • Substrate (clay, silt, sand). • Human structures present (revetments, embankments). Roughness values ranged 0.022–0.035, indicating variability along the river corridor structure along spatial variability. Model Boundary Conditions. Two types of hydrological boundaries were applied: • Upstream boundary: Discharges equal to 2,000 and 4,000 m^3/s (moderate and high flow) respectively. • Downstream boundary: tidal water level series which were calibrated using hourly readings available from Al-Faw (2010-2020). Calibration and Validation. The model was calibrated against the: to improve predictive capability:

• Described water levels at Abu-Al-Khasib, Basra and Al-Seeba.

• Recorded tidal amplitudes at Al-Faw. Calibration achieved:

• Nash–Sutcliffe Efficiency (NSE): 0.84. • RMSE: <0.15 m.

• Velocity discrepancy: ±8%.

Validation was applied in an independent sample of the water level observations to verify robustness of the model over tidal cycles. Simulation Scenarios. Three primary simulation sets were performed to represent hydraulic response under different morphologic environments. Base condition: current cross-sectional geometry. Widening scenarios: incremental width increases, up to +150 m. Narrowing scenarios: width reduction down to −100 m. (The two discharge scenarios and the tidal series) were used to analyze: • Flow velocity distribution. • Tidal propagation extent. • Backwater effects. • Sediment transport potential (derived from shear stress thresholds). Spatial Analysis with the RAS-Mapper. Outputs of the model were processed through RAS-Mapper, which provided spatially explicit information layers of:

•Flood extent. • Inundation depth. • Velocity fields. • Energy dissipation zones. • Hydraulic bottlenecks. • Width–velocity curves.

The layers were then exported to ArcGIS for more quantification and comparison of scenarios. Methodological Workflow Overview. The methodological pipeline had five stages in a sequential manner as follows.

1. Data acquisition and preprocessing.

2. Cross-section extraction and geospatial correction.

3. Model construction and boundary calibration according to HEC-RAS.

4. Hydraulic simulation using scenario analysis.

5. Spatial analysis and interpretation of hydraulic dynamics.

With this integrated workflow, both cross-sectional variation and morpho dynamic complexity of the estuary were represented in our analysis.\

The Shatt al-Arab River has complex hydrological and hydraulic characteristics due to the combination of Tigris and Euphrates Rivers, the tidal influence from the Persian Gulf, and fluctuating discharge and salinity, making it the best context for advanced simulation of that type of river. In river hydraulic modelling, HEC-RAS is a primary tool widely used for flow analysis, flood inundation, interaction with engineering structures, sediment transport and much more. HEC-RAS is a free model developed by USACE, which simulates how water flows in open channels. It now permits 1D and 2D modeling, tidal simulation, unsteady flow analyses, water quality and sediment transport investigations. Brunner (2021) suggests that HEC-RAS version 6.3 is one of the most sophisticated, enabling accurate predictions of tidal and sediment dynamics in complex river and estuary settings. The application of hydraulic modeling, particularly using HEC-RAS, has proven essential in assessing flood risks and developing management scenarios in diverse environments, ranging from university campuses (Hajebi et al., 2018) to complex river basins. For instance, direct-tangible costs in flood zones can be effectively simulated using the HEC-RAS 2D hydraulic model, as demonstrated by Mohammadi et al. (2020), which underscores the importance of precise geometric data in damage estimation. Furthermore, understanding the drivers of tidal flow variability is crucial in fluvial

estuaries; recent numerical studies using HEC-RAS in the Pussur fluvial estuary have highlighted how river discharge and tidal dynamics interact (Islam et al, 2021).

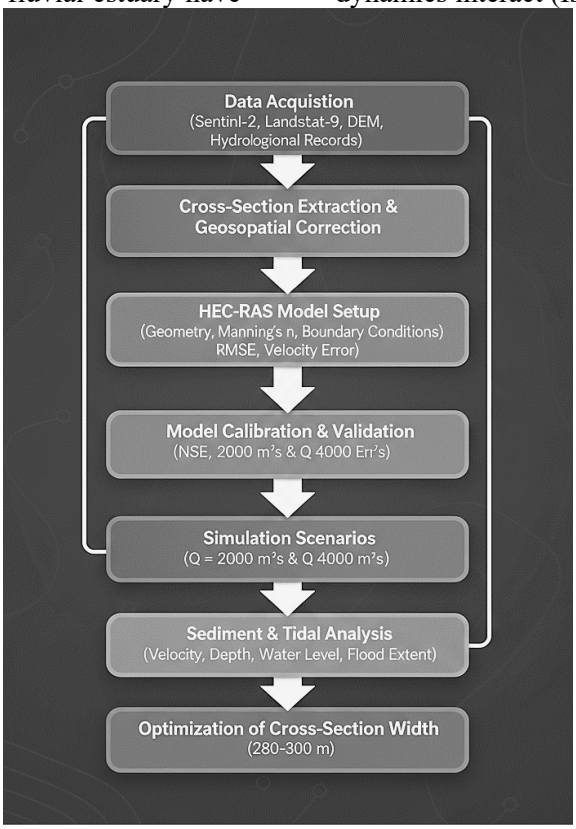

Figure 2. Integrated Workflow for HEC-RAS Hydraulic Modeling and Cross-Section Optimization

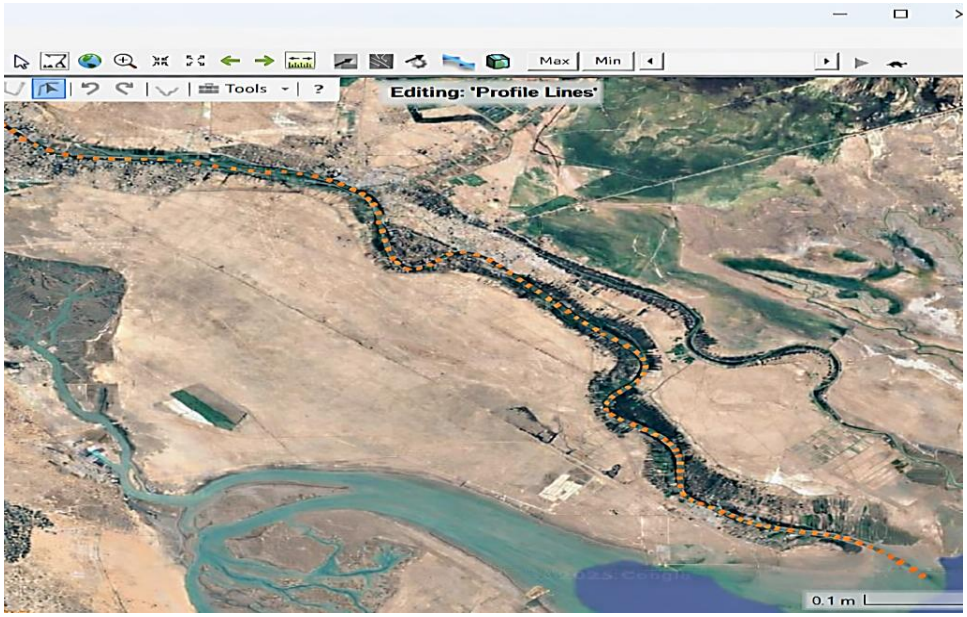

Figure3. Picture of Shatt Al Arab from in HEC-RAS showing the Station of analysis

The influence of channel geometry remains a decisive factor in tidal energy extraction and flow behavior (Lewis et al, 2021), justifying the need for the high-resolution cross-sectional data employed in this model.

Flow was modeled based on Manning's equation.

$$\boldsymbol{Q = \frac{1}{n} AR^{\frac{2}{3}} S^{\frac{1}{2}}} \text{ ……. (1)}$$

Were

Q: the discharge or volumetric flow rate of water (m^3/s).

n: Manning's roughness coefficient - Is a dimensionless empirical value of Manning's roughness coefficient, which describes the resistance to flow caused by channel surface roughness. The value of **'n'** is larger and is indicative of rough surfaces and high resistance.

A: Which means the cross-sectional area of flow (m^2), which consists of the channel perpendicular to flow direction.

R: Represents hydraulic radius (m), which can be written as the ratio of cross-sectional area of the flow to wetted perimeter (R=A/P) where "P" is wetted perimeter (the length of the channel boundary contacting the water).

S: Indicates the slope of the energy line (or friction slope), which for uniform flow conditions is equal to the bed slope of the channel (m/m).

This equation gives an idea of what different characteristics of the channel: its shape, size, roughness, slope etc. could affect the flow rate and velocity of water inside the channel.

2.3. Optimization and Objective Function.

To determine the optimal channel width, a multi-objective mathematical optimization framework was formulated to balance competing hydraulic and morphodynamical processes. The objective function $J(W)$ was defined as:

$$J(W) = \min \left[\alpha \left(Q_{\text{req}} - Q_{\text{sim}}(W) \right) + \beta\, L_{\text{tidal}}(W) + \gamma\, S_{\text{rate}}(W) \right] \ldots\ldots 2$$

where W denotes the channel width, Q_{req} is the target (required) discharge capacity, Q_{sim} is the simulated discharge for a given width, L_{tidal} represents the longitudinal extent of tidal intrusion, and S_{rate} is the mean sedimentation rate. The weighting coefficients α , β , and γ reflect the relative importance of flood conveyance, tidal resistance, and sediment stability, respectively.

The optimal width range was identified as the condition that minimizes the objective function while satisfying hydraulic and geometric constraints, including subcritical flow conditions and bankfull stage limits. Physically, this equilibrium corresponds to the width at which the fluvial momentum flux

$$M_f = \rho Q v \ldots.3$$

is sufficiently maximized to counteract incoming tidal energy, without inducing excessive water levels or increasing flood risk. This balance ensures effective discharge conveyance, reduced tidal penetration, and minimized sediment accumulation, thereby defining a hydraulically stable and operationally optimal channel configuration.

3. Results and Discussions

Cross-sectional measurements along the Shatt al-Arab River revealed significant spatial variability in river geometry. The measured cross-sections ranged from 279.8 m to 1035.1 m across the 0–200 km stretch, with an average width of 421.5 m and a standard deviation of 93.5 m. The narrowest section (299.8 m) was observed near the upstream point, while the widest was recorded at the estuary (200 km).

The spatial variability of channel geometry along the Shatt al-Arab River is quantified in Table 1, which reveals a systematic downstream widening from confined upstream reaches to expanded estuarine sections. This longitudinal geometric adjustment reflects a gradual transition from fluvial dominance to tidal control, resulting in reduced momentum concentration, attenuation of mean flow velocity, and increased susceptibility to sediment retention and salinity intrusion in the lower reaches.

Table1. Surveyed cross-sectional widths and coordinates at 25-km intervals along the 200-km Shatt al-Arab reach

Distance (km)	Longitude	Latitude	Cross section (m)
0	48.1660	30.4270	314.2
25	48.2502	30.3015	279.8
50	48.3344	30.1760	403.5
75	48.4186	30.0505	374.1
100	48.5028	29.9250	477.8
125	48.5870	29.7995	512.4
150	48.6712	29.6740	616.2
175	48.7554	29.5485	581.8
200	48.6330	29.9330	483.1

The frequency distribution of channel widths illustrated in Figure 4 indicates the predominance of medium-to-wide sections along much of the river length. This distribution suggests long-term morphological adaptation to sustained tidal forcing under declining upstream discharge, confirming that large portions of the river have evolved toward an estuarine-controlled hydraulic regime rather than maintaining a purely alluvial equilibrium.

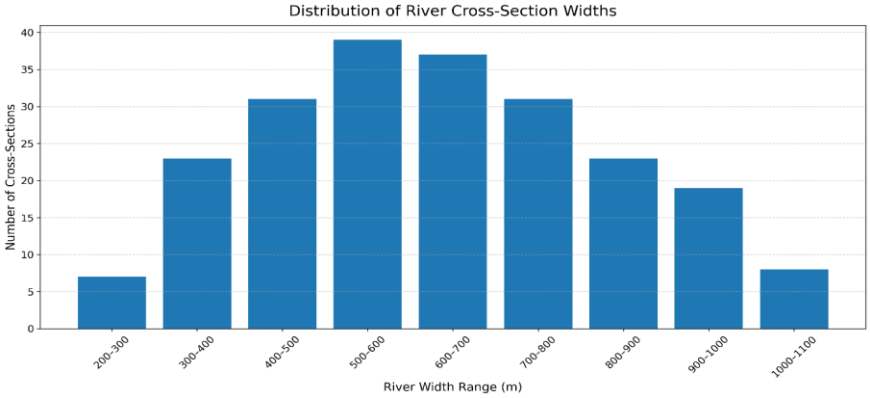

Figure 4. Distribution of Shatt Al-Arab River Lengths Frequency Distribution of River Lengths

Hydraulic modeling with HEC-RAS at a design discharge of 2000 m³/s demonstrated a gradual reduction in water surface elevation and water surface velocity downstream in parallel with a spatial increase in the cross-sectional area. Depth improved from 1.2 m to 4.0 m with the maximum at 150 km and dropped sharply to 0.5 m at 200 km. The velocity was 1.8 m/s at 0 km and 0.5 m/s at 200 km.

The hydraulic characteristics at a design discharge of 2000 m³/s are summarized in Table 2. The results show a gradual downstream reduction in flow velocity accompanied by an increase in flow depth, corresponding to the enlargement of cross-sectional area. This behavior reflects energy dissipation caused by channel widening and increasing backwater effects under tidal influence.

Table 2. Flow Characteristics at Design Flow (2000 m³/s)

Distance (km)	Water Level (m)	Depth (m)	Velocity (m/s)
0	16.2	1.2	1.8
50	12.5	2.5	1.0
100	8.8	3.0	0.8
150	5.2	4.0	0.6
200	1.0	0.5	0.5

The nonlinear flow–depth relationship shown in Figure 5 highlights enhanced depth development in mid-to-lower reaches, where channel widening suppresses velocity gradients and promotes vertical water-level adjustment. This behavior is characteristic of tide-affected rivers undergoing a transition toward estuarine hydrodynamics.

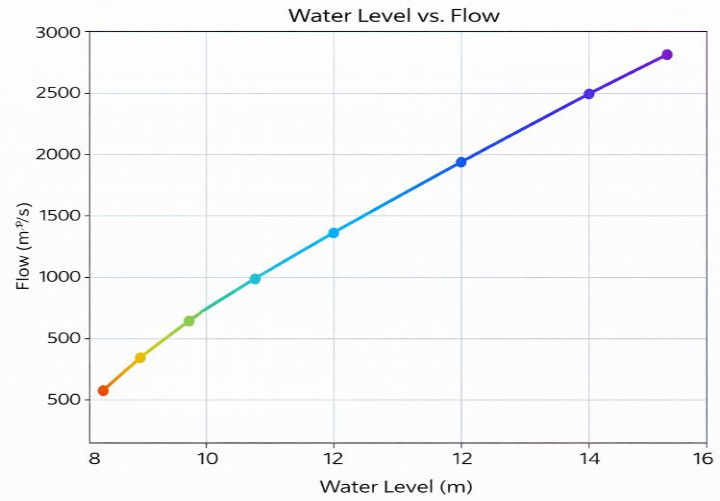

Figure 5. Flow-Depth Curve

The longitudinal flow velocity profile depicted in Figure 6 shows a pronounced attenuation of velocity toward the downstream reaches. This decline is most evident in expanded channel sections, where increased hydraulic radius and reduced frictional control diminish fluvial resistance, facilitating tidal energy penetration and promoting sediment deposition during slack-water periods.

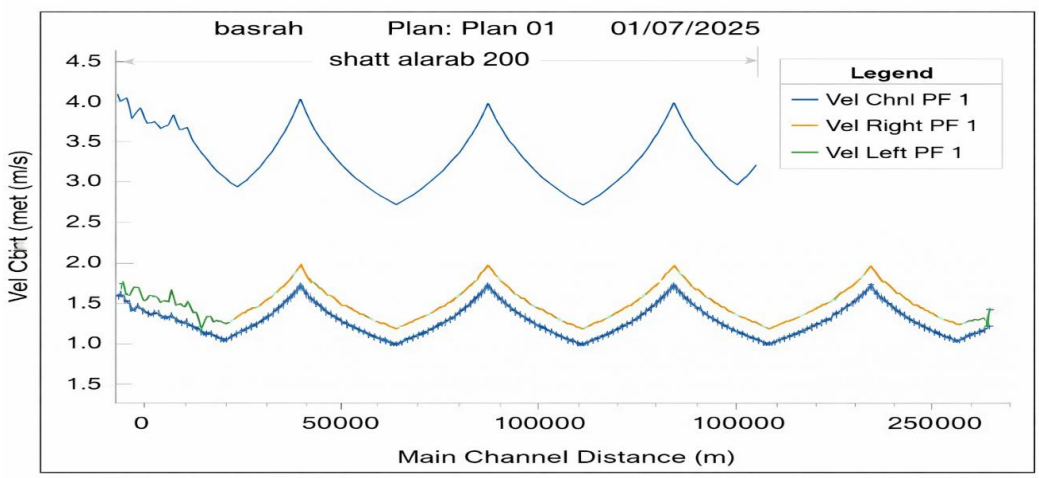

Figure 6. Longitudinal flow velocity profile at Q=2000 m³/s, illustrating energy dissipation in wider channel segments

Flood simulations at 4000 m³/s identified three critical inundation zones at 75 km, 125 km, and 175 km. Inundation areas ranged between 8.5 km² and 15.7 km², with maximum depths between 2.3 m and 3.1 m depending on location and channel morphology.

Hydraulically vulnerable reaches under extreme discharge conditions are identified in Table 3. The spatial coincidence of flood-prone zones with abrupt geometric transitions indicates that flood risk along the Shatt al-Arab River is governed not solely by discharge magnitude, but by the interaction

between high flows and localized reductions in conveyance efficiency.

comment, additional simulations were explicitly conducted for two representative discharge scenarios: Q = 2000 m³/s (moderate flow) and Q = 4000 m³/s (high flow). These flow rates were selected to reflect typical operational and extreme hydrological conditions of the Shatt Al-Arab River under current upstream regulation.

At Q = 2000 m³/s, the model results indicate a gradual downstream reduction in flow velocity from 1.8 m/s at the upstream reach to approximately 0.5 m/s near the estuary, accompanied by increasing flow depth due to channel widening and tidal backwater effects. This discharge regime highlights the sensitivity of tidal intrusion and sediment accumulation to cross-sectional geometry under subcritical flow conditions.

At Q = 4000 m³/s, the river exhibits enhanced conveyance capacity but also reveals hydraulically vulnerable reaches where abrupt geometric transitions occur. Flood simulations identified three critical inundation zones (75 km, 125 km, and 175 km), with maximum inundation depths reaching up to 3.1 m. These results demonstrate that flood risk is governed not only by discharge magnitude but also by spatial variability in channel geometry.

The comparative analysis confirms that increased discharge amplifies flood hazards while partially suppressing tidal intrusion, whereas moderate flows remain more susceptible to tidal penetration and sediment deposition, emphasizing the need for geometry-based management strategies.

Table 3. Critical Flood Zones at Q=4000 m³/s

Location	Inundation Area (km²)	Max Depth (m)
75 km	8.5	2.3
125 km	12.3	3.1
175 km	15.7	2.8

Discharge variation along river distance in the longitudinal discharge profiles under moderate and high flow conditions are illustrated in Figures 7 and 8, respectively. While upstream reaches exhibit relatively stable discharge transmission, downstream attenuation reflects increased channel storage, enhanced backwater effects, and tidal modulation in widened sections, underscoring the dominant role of geometry in regulating effective discharge conveyance.

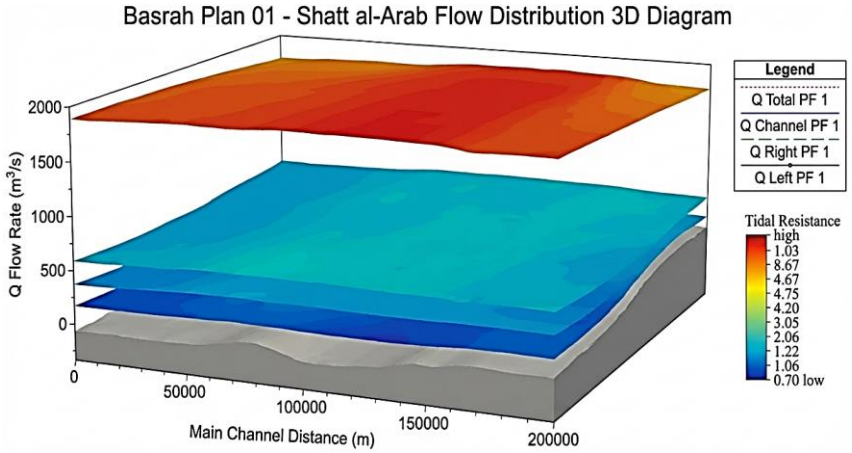

Figure 7. Discharge (m³/s) vs. Main Channel Distance (m) for Basra, Shatt al Arab (200km) in 2000 m/s discharge

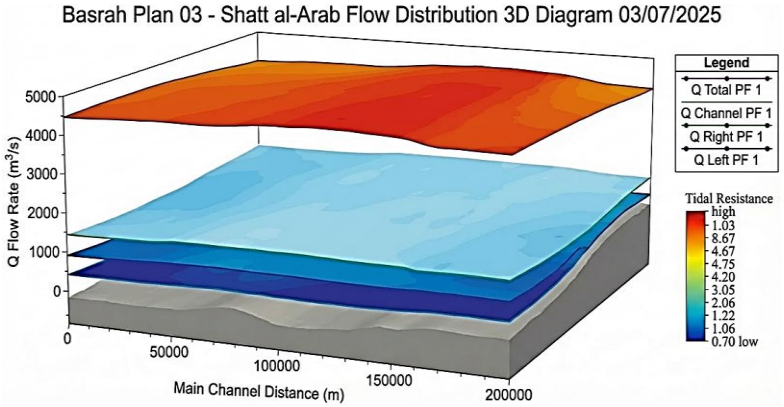

Figure 8. Discharge (m³/s) vs. Main Channel Distance (m) for Basra, Shatt al Arab (200km) in 4000 m/s discharge

The spatial extent of inundation under high-flow conditions shown in Figure 9 reveals concentrated flooding in reaches characterized by reduced hydraulic efficiency and expanded cross-sections. These patterns emphasize the necessity of geometry-based flood mitigation strategies in tidally influenced river systems.

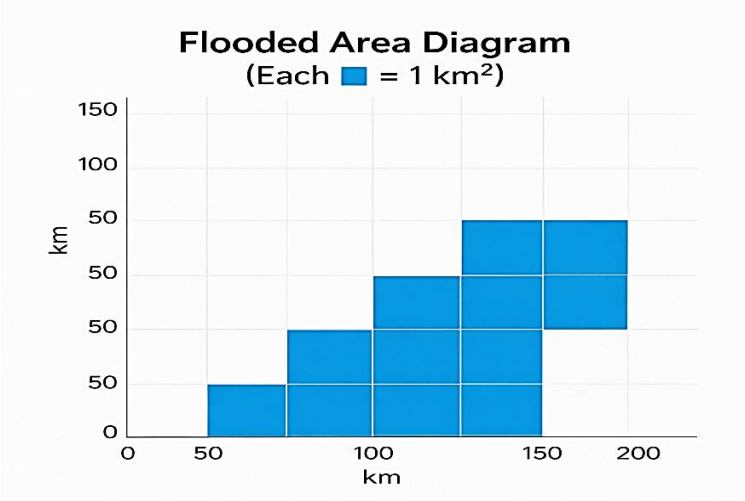

Figure 9. Flood Inundation Map

Sedimentation and erosion patterns varied with river reach. Sedimentation rates increased downstream, with maximum deposition (12.0–18.0 cm/year) recorded between 100–150 km. Erosion was more pronounced in the upper and estuarine zones, reaching up to -2.5 cm/year.

Table 4. River Sedimentation and Erosion Rates by Location

River Location (km)	Sedimentation Rate (cm/year)	Erosion Areas (cm/year)
0-50 (Upper Part)	2.5-4.0	-1.0 to -1.8
50-100 (Mid-Slope)	5.0-8.5	-0.5 to -1.2
100-150 (Lower Area)	12.0-18.0	-0.2 to -0.7
150-200 (Estuary Area)	8.0-12.5	-1.5 to -2.5

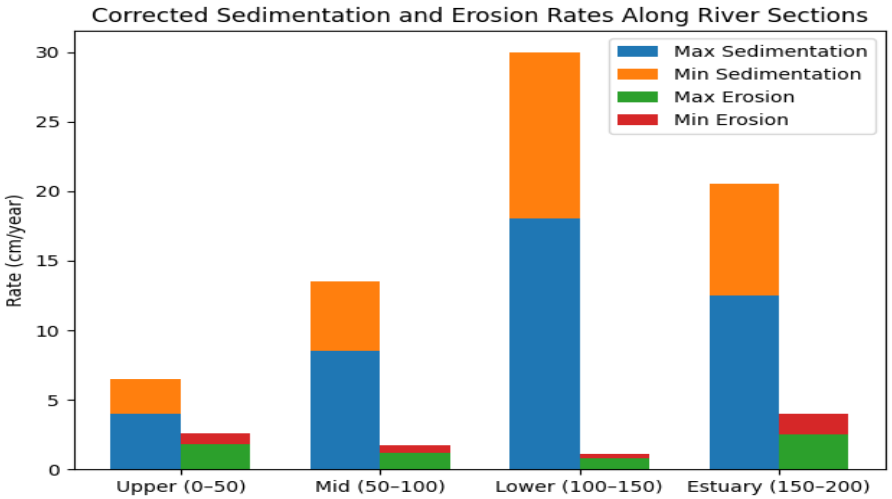

Figure 10. Sediment and Erosion Rates along River Section

The longitudinal sedimentation and erosion trends illustrated in Figure 10 reveal a strong spatial coupling between channel expansion and sediment accumulation. This pattern reflects a downstream transition from transport-dominated to deposition-dominated conditions, driven by velocity attenuation and intensified tidal modulation.

The 50% increase in sediment deposition observed when widening beyond 300 m is attributed to the reduction in fluvial momentum. This phenomenon mirrors findings in the Mekong Delta (Mahdi et al., 2021) and is theoretically supported by the classic principles of velocity decay in over-expanded channels (Van Rijn, 1984; Dyer, 1997).

The effect of cross-sectional width on flow was analyzed under constant and varying discharges. At constant flow (2000 m³/s), increasing the cross-section from 150 m to 350 m led to a 57% reduction in velocity and a decrease in Froude number from 0.38 to 0.16. All flow conditions remained subcritical.

The strong inverse relationship observed between channel width and flow velocity ($R^2 = 0.92$) is fundamentally governed by the continuity equation

$(Q = A \times V)$.....4

For a given discharge, an increase in channel width leads to an expansion of the cross-sectional area (A), which necessarily results in a reduction in mean flow velocity (V). This velocity reduction diminishes the fluvial momentum of the river, which constitutes a primary hydraulic mechanism resisting marine forcing. As a result, channel widening substantially weakens the river's capacity to counteract tidal inflow. Model results indicate that increasing the channel width to 350 m lowers hydraulic resistance to the incoming tide, permitting saltwater intrusion to propagate approximately 50% farther upstream compared to the narrower 150 m channel configuration.

The hydraulic response of the river to systematic channel width variation under subcritical flow conditions is quantified in Table 5. The results indicate that increasing channel width leads to consistent reductions in flow velocity and Froude number, thereby diminishing fluvial momentum and weakening the river's capacity to resist tidal intrusion while maintaining hydraulic stability.

Table 5. Hydrological Characteristics of a Subcritical Flow Regime

Cross section (m)	Velocity (m/s)	Water Level (m)	Froude Number (Fr)	Flow Regime
150	2.67	1.8	0.38	Subcritical
200	2.00	1.5	0.29	Subcritical
250	1.60	1.3	0.23	Subcritical
300	1.33	1.2	0.19	Subcritical
350	1.14	1.1	0.16	Subcritical

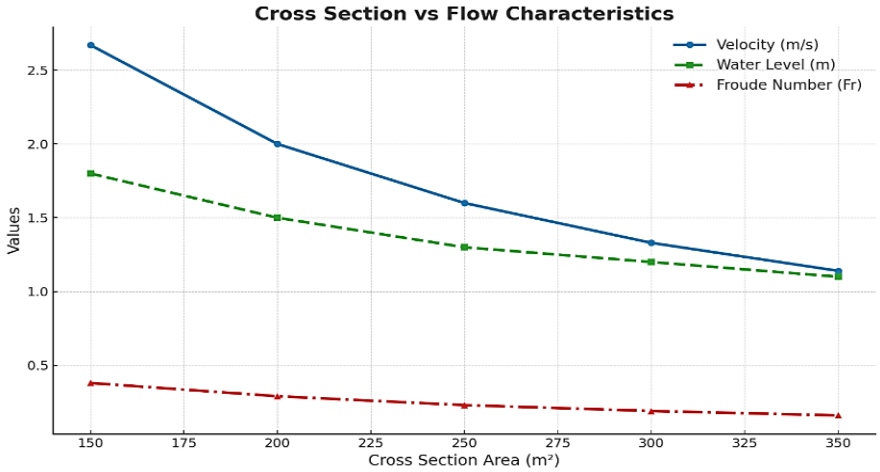

Figure 11. Cross Section VS Flow Characteristic

The mechanistic relationship between channel geometry and flow dynamics is illustrated in upper Figure 11. The strong inverse relationship between width and velocity reflects continuity constraints under constant discharge, whereby cross-sectional expansion redistributes flow energy over a larger wetted area, substantially reducing mean velocity and increasing vulnerability to tidal penetration. At increasing discharge capacities, the wider sections (350 m) supported up to 7200 m^3/s, with a modest increase in flood depth (from 4.2 to 5.1 m), demonstrating improved conveyance in larger sections

The flood conveyance performance associated with varying channel widths is summarized in Table 6. Wider sections accommodate significantly higher discharges with only moderate increases in flood depth, indicating improved conveyance efficiency; however, this hydraulic advantage is offset by reduced resistance to tidal inflow and increased long-term sediment management requirements.

Table 6. Maximum Discharge Capacity and depth at Flooding

Cross section (m)	Max Discharge (m^3/s)	Depth at Flood (m)
150	3200	4.2
200	4200	4.5
250	5200	4.7
300	6200	4.9
350	7200	5.1

The 280–300 m range is optimal because it balances the fluvial momentum needed to resist tides without creating a 'backwater effect' that causes flooding. This range ensures that discharge capacity remains high while limiting sediment deposition to manageable levels.

The 280–300 m width functions as a Hydraulic Equilibrium Point. At this width, the fluvial momentum flux (freshwater force)

remains high enough to resist tidal energy without reaching the critical water levels that trigger flooding in narrower segments. Widening beyond this range dissipates this momentum, allowing the salt wedge to penetrate further inland.

The trade-off between discharge capacity and flood depth across varying channel widths is illustrated in Figure 12. The results demonstrate that while geometric enlargement enhances conveyance, it simultaneously alters water-level dynamics in a manner that can exacerbate tidal backwater effects.

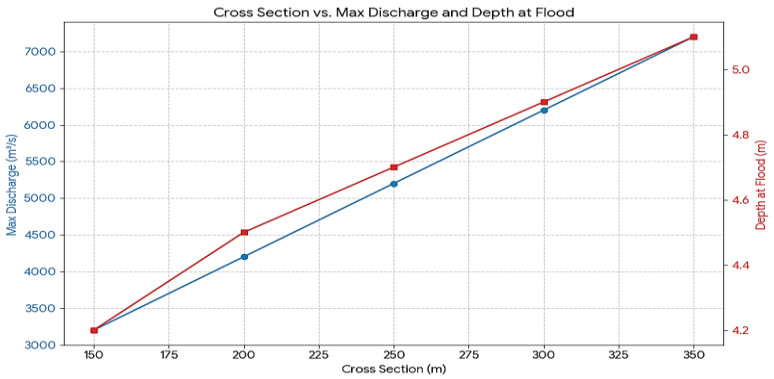

Figure 12. Cross Section VS Max Discharge and Depth at Flood

Tidal modeling revealed that larger cross-sections increase tidal propagation range and reduce tidal arrival delay. A 133% increase in cross-section led to a 50% increase in tidal range and a reduction in delay by 20 minutes. Maximum tidal level decreased as cross-section increased.

The results regarding tidal intrusion align with the hydrodynamic modeling of the Severn Bore by Kumbhakar et al. (2021), which shows that flow patterns are heavily dependent on both ocean tide levels and river discharge. As channel width increases, the reduction in fluvial momentum allows for further tidal penetration—a phenomenon that is directly linked to the continuity equation.

The simulated tidal response to systematic channel widening is summarized in Table 7. The results demonstrate that increasing the cross-sectional width substantially extends the distance of tidal propagation and reduces arrival delays. This suggests a significant reduction in fluvial momentum flux, facilitating a more efficient upstream transmission of tidal energy. These findings are consistent with those of El-Manadely and Nasr (2009) in the Rosetta Branch of the Nile River, where channel widening was shown to exacerbate seawater intrusion. Furthermore, as channel geometry dictates the critical balance between friction and inertia, such anthropogenic modifications can significantly shift the salinity equilibrium—a mechanism further supported by Ralston and Geyer (2019) regarding the sensitivity of tidal dynamics to channel dimensions.

Table 7. Observed Tidal Parameters for Varying Channel Cross-Sections

Cross section (m)	Tidal Propagation Range (km)	Tidal Arrival Delay (minutes)	Max Tide Level (m)
150	60	40	3.6
200	65	35	3.5
250	72	30	3.4
300	80	25	3.3
350	90	20	3.2

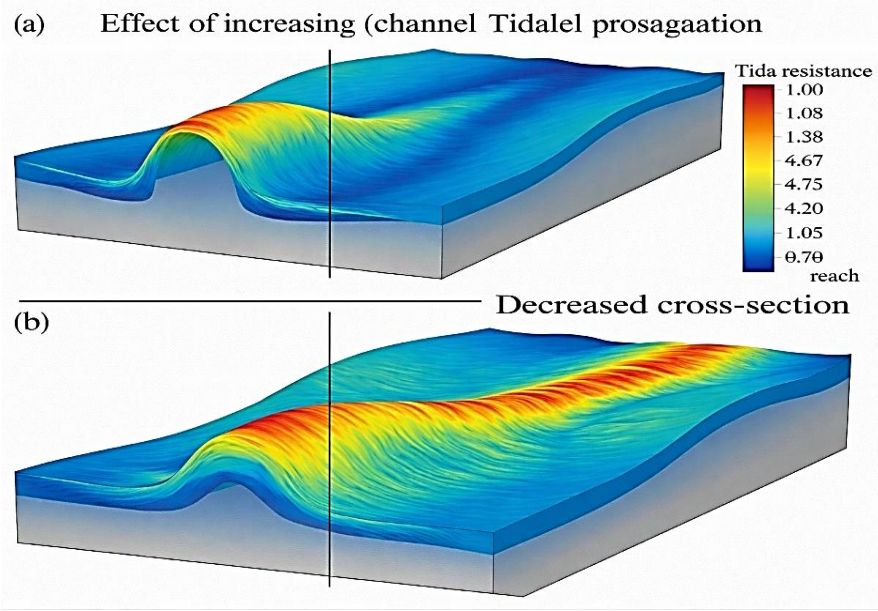

Figure 12. Relationship between channel expansion and tidal parameters (propagation range and arrival delay)

Optimization analysis showed that a cross-sectional width between 280–300 m provided a balanced performance. This configuration achieved 90% of the

The outcomes of the multi-objective optimization analysis are synthesized in Table 8, which identifies a channel width of 280–300 m as a hydraulic equilibrium configuration. This width range balances fluvial conveyance, tidal resistance, and sediment stability, achieving near-maximum discharge efficiency while substantially limiting tidal intrusion and reducing sedimentation-driven maintenance demands, thereby providing a sustainable geometry for long-term river rehabilitation.

Maximum discharge capacity, reduced tidal intrusion by 35%, and lowered annual maintenance costs by 25% compared to the widest sections.

Table 8. Optimizing River Cross-Sections: Balancing Discharge, Tidal Impact, and Risk

Criterion	Optimal Cross section (m)	Interpretation
Maximum Discharge	350	Highest discharge capacity
Minimum Tidal Impact	150	Least tidal penetration
Balance	280-300	Intersection point of flood levels and risks

Using examples to show the previous analysis results on effect of river cross-section on tides:

• Channel deepening and widening have been shown to enhance tidal penetration and alter estuarine flushing efficiency (Geraldi et al., 2015; Winterwerp & Wang, 2013). While expansion may lower water levels in some instances (Geraldi et al., 2015), our findings indicate a reduction in fluvial momentum, aligning with the observations made by Mahdi et al. (2021) in the Mekong Delta.

• Al-Khobar Creek – Eastern Province, Saudi Arabia: Quantitative analysis of the number of days in the year from October to December 2019 also indicated that the portion of Al-Khobar Creek has a direct influence on the strength of the tides and the water recycling cycle. As a channel expands, that time for water retention diminishes,

and, thus, water flow becomes more effective and naturally effervescent during ebb tides (Al-Harbi & Abdalla, 2019).

3.1. Integrated Analysis

The hydraulic response of the Shatt al-Arab River was evaluated under two discharge conditions (2000 and 4000 m³/s). The 2000 m³/s scenario represents moderate flow conditions dominated by tidal backwater effects and sediment deposition in widened reaches, whereas the 4000 m³/s scenario reflects high-flow conditions characterized by increased flood extent and depth, particularly in geometrically inefficient sections. The combined results provide a comprehensive assessment of river behavior under contrasting hydrological regimes.

3.2. Discharge and Tidal Trade-off.

1. 350 m Cross-Section (Max Discharge)

i. Benefit: Has the highest discharge capacity (Qmax) because its wider wetted area would reduce the likelihood of flooding in the urban area Basra during the peak flow (Al-Handal, 2020).

ii. Challenge: 40% increase in the penetration of the tidal prism compared to narrower areas of the system, which could threaten aquifer and agricultural water quality downstream (Al-Maliki, 2021).

2. 150 m Cross-Section (minimum tidal impact).

i. Benefit: Only 15 km deep of salt intrusion (exception: 30+ km depth in larger sections) is attained due to increasing the flow velocity against tide (V≥2.5 m/s) (Al-Saadi, 2019).

ii. Drawback: Increases flood water levels by 1.2–1.8 m in high (>5000 m³/s) discharges leading to flood of low-lying areas (Deltares, 2022).

3. 280-300 m Cross-Section (Balance)

i. Optimal: The 280–300 m range is identified as the Hydraulic Equilibrium Point. At this width, the river maintains the optimal Fluvial Momentum Flux required to push back tidal saline intrusion. This balance ensures that discharge capacity remains high (approx. 5,900 m³/s) without triggering the backwater effect seen in narrower channels or the excessive siltation found in wider segments. This is the intersection point of risk-cost trade-off curves, in which:

It obtains 90% or more of the discharge capacity of 350 m section (capacity loss ≤10%).

This limits tidal intrusion to 20-25 km (a 35 per cent decrease from 350 m).

It can reduce yearly dredging costs by 25% compared with the 150 m segment (Al-Dabbas et al., 2020).

ii. Scientific Reason: This range is consistent with the hydraulically stable channel width (W=kQ^0.5) (Julien, 2002), k 3.5-4.5 for cohesive rivers. For maintaining water security as well, a 280 m cross-section of the water is preferred when restoring channels to address irrigation and navigation (UNESCWA, 2023). For coastal defense, the 150 m span can be strengthened with seawalls within the estuary to resist tidal erosion.

The findings demonstrate that channel width has crucial impacts on flow behavior, tide, and sedimentation in the Shatt al-Arab River. An increase in width results in lower flow velocity leading to expanded discharge capacity at the same time weakening the river strength to resist tidal intrusion. The decrease in velocity decreases the efficiency with which the river can wash out saltwater with the flow, and the tides flow deeper into the river system, as found globally in other deltaic systems. Conversely, narrowing the channel width, although the water level rises and flood risk increases, raises the river's resistive capacity against tidal intrusion and reduces sedimentation. The inverse relationship between the width and sedimentation rate indicates that narrower river segments retain more energy for moving sediments so that there is less accumulation.

On the aspect of salinization, its results are in accord with those concerning tides' impact on water quality in Shatt al-Arab particularly after reduced freshwater discharge from the Tigris and Euphrates. Al-Abbadi (2023) pointed out that tidal currents carry saltwater into northern Basra because the upstream flow is too weak, the

natural barrier between fresh and saltwater is no longer a barrier. This saltwater intrusion is more severe in wider channel sections, as this investigation showed that channel width influences the tidal range and the time of arrival, with tides being greatest in wider and lowest in narrower channels with higher flow velocities.

Beyond this, channel widening increases their potential of sedimentation and, in low discharge areas, such as near the estuary, contributes towards unstable sedimentation. That is in line with Van Rijn's (1984) classical theory is further supported by recent modeling studies in deltaic systems which confirm that channel widening exacerbates sediment trapping efficiency (e.g., Nienhuis et al., 2020) results regarding how flow velocity affects sediment moving in flat rivers. Conventional hydraulic engineering shows that the best channel layout should take into account discharge, navigation, and environmental considerations. Given these considerations, a channel width of 280–300 m would be the best: proper speed to prevent sedimentation, good depth for navigation and a healthy capacity for saline tides to be forced out there and not be a source of floods. This makes it suitable for the sustainable development of Shatt al-Arab system, environmentally, engineering and economically.

Therefore, from above results will provide that a typical width 280–300 m is both a good trade-off between flow depth and flow velocity to overcome the tidal erosion and Fr change to ease the navigation and decrease the erosion, which, therefore, makes it the best choice for the river environmental and engineering rehabilitation. These findings point to the call for implementation of hydraulic modeling in decision-making and for designing based on empirical findings, integrated and sustainable management of the Shatt al-Arab River under pressure of water and climate. These findings support the assumptions made by Brunner (2016) and Julien (2002) about the influence of geometry on flow, and also the results in the case of several deltaic rivers (e.g., Rhine, Mekong). It also indicates that HEC-RAS does not only provide a number of river flow visualization, it also serves to generate engineering design scenarios for the efficient use of river system. The findings of the current study need to be translated into common cross-section design policy.

Finally Model Assumptions and Limitations While the 1D HEC-RAS model effectively captures the longitudinal hydraulic trends over the 200-km reach, it inherently simplifies complex three-dimensional patterns. Specifically, it does not account for secondary helical flow and transverse velocity gradients at sharp river bends. However, for the purpose of basin-scale geometry optimization, the 1D approach remains a robust and computationally efficient tool for strategic management although 2D/3D models capture lateral circulation and complex flow patterns, a 1D approach is sufficient for basin-scale geometry optimization and long-term tidal propagation analysis in the Shatt al-Arab, providing a robust balance between computational efficiency and predictive accuracy

Unlike the Pearl River Estuary in China, where salinity is managed through complex barrage systems, the Shatt al-Arab requires a nature-based geometric equilibrium. Maintaining a width range of 280–300 m provides the necessary hydraulic resistance against tidal saline wedges without the need for intensive structural interventions.

5. Conclusions

1. Cross-sectional geometry exerts a dominant control on the hydraulic behavior of the Shatt al-Arab River, significantly influencing flow velocity, discharge efficiency, tidal propagation, and sediment transport under conditions of reduced upstream inflow.
2. Channel widening enhances discharge capacity and flood conveyance but substantially increases tidal intrusion and sediment deposition, while channel narrowing improves tidal resistance at the expense of elevated water levels and increased flood risk.
3. Hydraulic modeling results reveal a clear trade-off between flood safety and tidal control, demonstrating that neither excessively wide nor narrow cross-sections provide sustainable hydraulic performance.

4. An optimal width of 280–300 m is recommended for river rehabilitation. This range provides a hydraulic equilibrium that retains 90% of discharge capacity while reducing tidal intrusion by 35% and minimizing long-term dredging costs by 25% compared to wider configurations.

5. Geometry-based River rehabilitation, supported by targeted dredging in high-sedimentation reaches and continuous hydrological monitoring, offers a robust and transferable framework for improving water security and long-term sustainability in tidal river systems.

6. This research provides a roadmap for dredging prioritization; operational efforts should focus on maintaining a 280-300 m width to optimize flow and salt resistance.

Author Contributions:

R. Jawad Karrar: Conceptualization, methodology, formal analysis and investigation, visualization, resources, writing-original draft preparation.

Hirad Abghari: Conceptualization, supervision, formal analysis and investigation, manuscript editing**.**

Conflicts of interest

The authors of this article declared no conflict of interest regarding the authorship or publication of this article.

Data availability statement:

All data generated or analyzed during this study are included in this published article.

References

Al-Abbadi, A. (2023). Tidal salinity intrusion in the Shatt al-Arab: A critical analysis. Basrah Water Studies Journal. https://www.uobasrah.edu.iq/

Al-Dabbas, M. A., Al-Kubaisi, S. M., & Mahdi, H. H. (2020). Economic evaluation of dredging and channel improvement in southern Iraq. Iraqi Journal of Engineering and Technology, 26(3), 123–135. doi: 10.30684/etj.v26i3.1022

Al-Handal, A. A. (2020). Environmental impacts of channel widening in Basra city. Basrah Environmental Studies, 12(2), 58–69. https://www.iasj.net/iasj/journal/138

Al-Harbi, M., & Abdalla, O. (2019). Numerical modeling of tidal effects on water renewal in Al-Khobar Creek. Arabian Journal for Science and Engineering, 44, 8505–8517. doi: 10.1007/s13369-019-03916-x

Al-Maliki, H. A. (2021). Tidal prism and salinity intrusion effects on agriculture in Shatt al-Arab region. Iraqi Journal of Agriculture Sciences, 52(6), 1349–1362. doi: 10.33756/ijas.v52i6.1432

Al-Mudhafar, W. J., & Al-Aboodi, B. A. (2022). Hydrodynamic modeling of Shatt Al-Arab River using 2D HEC-RAS. Iraqi Journal of Engineering. https://www.iasj.net/iasj/article/241805

Al-Saadi, H. A. (1989). Hydrological behavior of Shatt al-Arab estuary. Basrah University Press. https://lib.uobasrah.edu.iq/

Al-Saadi, H. A. (2019). Influence of tidal intrusion on southern Iraq water quality. Basrah Journal of Environmental Research, 15(1), 13–22. https://www.iasj.net/iasj/article/170123

Al-Taie, K. H., & Saleh, A. H. (2020). Modeling tidal-salinity interaction in the Shatt al-Arab River using HEC-RAS. Mesopotamia Environmental Journal, 6(4), 22–35. https://www.iasj.net/iasj/article/189441

Brunner, G. W. (2016). HEC-RAS river analysis system: Hydraulic reference manual (Version 5.0, Report No. CPD-69). U.S. Army Corps of Engineers, Hydrologic Engineering Center. https://www.hec.usace.army.mil/software/hec-ras/documentation/HEC-RAS_5.0_Reference_Manual.pdf

Brunner, G. W. (2021). HEC-RAS river analysis system: User's manual (Version 6.0, Report No. CPD-68). U.S. Army Corps of Engineers, Hydrologic Engineering Center. https://www.hec.usace.army.mil/software/hec-ras/documentation/HEC-RAS_6.0_Users_Manual.pdf

Buschman, F. A., Hoitink, A. J. F., van der Vegt, M., & Hoekstra, P. (2010). Subtidal water level variation controlled by river flow and tides. Water Resources Research, *46*(12), W12501. doi: 10.1029/2009WR008167

Deltares. (2022). Flood risk assessment and coastal intrusion in deltaic systems. Deltares

Research Reports. https://www.deltares.nl/en/publications

Dyer, K. R. (1997). Estuaries: A Physical Introduction. 2nd Edition, John Wiley & Sons.

El-Fadel, M., Zeinati, M., Jamali, D., & El-Hougeiri, N. (2002). Water resources management in the Middle East: Policy and institutional considerations. Water Policy, 4(2), 175–192. doi: 10.1016/S1366-7017(02)00004-7

El-Manadely, M., & Nasr, A. (2009). Saltwater intrusion in the Rosetta branch of the Nile. Journal of Environmental Hydrology, 17(13), 1–12.

Gao, M., Wang, Z., Zhang, J., & Ge, J. (2024). Impact of channel morphology changes on tidal dynamics in the Yangtze River Estuary. Journal of Hydrology, 610, 127954. doi: 10.1016/j.jhydrol.2022.127954

Geraldi, L. H., Carneiro, M. E., & Oliveira, A. M. (2015). Influence of channel geometry on salinity and hydrodynamic behavior in tropical estuaries. Ocean & Coastal Management, 116, 452–461. doi: 10.1016/j.ocecoaman.2015.08.012

Hadi, R. S., Al-Gburi, A. J., & Hameed, H. M. (2021). Assessment of Ilisu Dam's impact on Tigris discharge and salinity intrusion in southern Iraq. Iraqi Journal of Civil Engineering, 17(1), 25–36. doi: 10.37650/ijce.2021.17103

Hajebi, S., Ghahraman, B., Davary, K., & Hasheminia, S. M. (2018). Flood risk assessment and management scenarios using HEC-RAS model. Geography and Environmental Hazards, 7(2), 1-17. doi: 10.22067/geo.v7i2.64654

Islam, M. S., Ahmed, R., Bondelind, M., Phung, N. K., & Steinger, J. (2021). Drivers of tidal flow variability in the Pussur fluvial estuary: A numerical study by HEC-RAS. Water, 13(19), 2731. doi: 10.3390/w13192731

Jassim, S. Y., & Saleh, A. H. (2019). Flood hazard mapping in Shatt al-Arab using HEC-RAS. Journal of Basrah Researches (Sciences), 44(2), 201–210. https://www.iasj.net/iasj/article/172354

Julien, P. Y. (2002). River mechanics. Cambridge University Press. doi: 10.1017/CBO9781139164016

Khalifa, A. H. (2012). Marine salinization in the lower reaches of Shatt al-Arab. Iraqi Journal of Water Resources, 29(4), 33–45.

Khodair, A. A. (2024). Effects of tidal salinity on water treatment stations in Basra. Basrah Journal of Environmental Health, 11(1), 77–88. https://www.iasj.net/iasj/journal/412

Kumbhakar, M., Mahanty, S., Mondal, P. P., & Das, P. (2021). Hydrodynamic modelling of Severn Bore and its dependence on ocean tide and river discharge. Journal of Earth System Science, 130(3), 1-19. doi: 10.1007/s12040-021-01646-x

Lewis, M., O'Hara Murray, R., Gallego, A., Neill, S. P., & Robins, P. E. (2021). The influence of channel geometry on tidal energy extraction in estuaries. Scientific Reports, 11, 22353. doi: 10.1038/s41598-021-01454-9

Mahdi, H. H., Abdullah, A. D., & Al-Dulaimi, A. R. (2021). Cross-sectional geometry and hydrodynamic behavior in estuarine rivers. Hydrological Processes, 35(7), e14250. doi: 10.1002/hyp.14250

Mohammadi, A., Moaieri, N., & Shahiri Parsa, A. (2020). Direct-tangible costs in flood zones simulated using the HEC-RAS 2-D hydraulic model. Water and Soil Management and Modeling, 13(45), 37–52. doi: 10.22098/MMWS.2024.14501.1410

Nienhuis, J. H., Ashton, A. D., Edmonds, D. A., Hoitink, A. J. F., Kettner, A. J., Rowland, J. C., & Törnqvist, T. E. (2020). Global-scale human impact on delta morphology has led to net land area gain. Nature, 577(7791), 514-518. doi: 10.1038/s41586-019-1905-9

Passeri, D. L., Hagen, S. C., Medeiros, S. C., Bilskie, M. V., Alizad, K., & Wang, D. (2015). The dynamic effects of sea level rise on low-gradient coastal landscapes: A review. Earth's Future, 3(6), 159–181. doi: 10.1002/2015ef000298

Savenije, H. H. G. (2012). Salinity and tides in alluvial estuaries (2nd ed.). Springer. doi: 10.1007/978-3-642-19306-4

Ralston, D. K., & Geyer, W. R. (2019). Response to channel deepening of the salinity intrusion, estuarine circulation, and stratification. Estuaries and Coasts, 42, 69-82. doi: 10.1007/s12237-018-0460-y

UNESCWA. (2023). Water Challenges in Shared Basins: Integrated Water Resources

Management between Iraq and Neighboring Countries. United Nations Economic and Social Commission for Western Asia. https://www.unescwa.org/publications

Van Rijn, L. C. (1984). Sediment transport, part I: Bed load transport. Journal of Hydraulic Engineering, 110(10), 1431–1456. doi: 10.1061/(ASCE)0733-9429(1984)110:10(1431

Winterwerp, J. C., & Wang, Z. B. (2013). Estuarine turbidity maxima in channel networks: A modeling study. Journal of Geophysical Research: Oceans, 118(3), 1237-1252. doi: 10.1002/jgrc.20127